

Chaos-Coded Modulations Over Rician and Rayleigh Flat Fading Channels

Francisco J. Escribano, L. López, and M. A. F. Sanjuán

Abstract—In this brief, we analyze a kind of chaos-coded modulations over both Rician and Rayleigh frequency non-selective uncorrelated fading in the presence of additive white Gaussian noise. We provide bounds both for the case when perfect channel-state information (CSI) is available at the decoder and when there is no CSI. We show that the bounds proposed can be tight enough to give reason of the behavior of these systems in a flat fading channel. We compare the results with a related trellis-coded modulation and show that the degradation in performance can be at least as low as with conventional coded modulation systems.

Index Terms—Chaos, error analysis, fading channels, modulation coding.

I. INTRODUCTION

SOME recent works have stressed the fact that chaos-coded modulation (CCM) systems working at a joint waveform and coding level can be efficient in additive white Gaussian noise (AWGN) [1], [2]. This contrasts with previous state of the art [3]. This success has been achieved by building a bridge linking the fields of chaos theory and digital communications. But there is still a need to evaluate these promising developments in other environments. That is why we address here the task to provide bounds on the bit-error rate (BER) for a whole kind of CCMs in flat fading channels. Chaos-based modulation systems working at the waveform level have already shown to be of potential use in multipath fading channels [4], as well as chaos-based systems working at the coding level [5]. Though we have chosen only some examples in order to show the results and the accuracy of the bounds, the principles shown can be straightforwardly applied to any CCM allowing a representation in terms of a trellis. The comparison with a conventional trellis-coded modulation (TCM) system allows us to foresee good possibilities for this kind of CCM in dispersive channels, where the bounds provided can be useful in design and evaluation tasks.

Manuscript received June 14, 2007; revised December 20, 2007. This work was supported by the Spanish Ministry of Science and Technology under Grant TSI2006-07799, by the Comunidad de Madrid under Grant S-0505/TIC/0285, and by Universidad Rey Juan Carlos under Project URJC-CM-2007-CET-1601. This paper was recommended by Associate Editor T. Schimming.

F. J. Escribano was with the Departamento de Física, University Rey Juan Carlos, 28933 Móstole, Spain. He is now with the Department of Signal Theory and Communications, Universidad Alcalá de Henares, 28805 Alcalá de Henares, Spain (e-mail: francisco.escribano@ieeee.org).

M. A. F. Sanjuán is with the Departamento de Física, University Rey Juan Carlos, 28933 Móstoles, Spain (e-mail: francisco.escribano@ieeee.org).

L. López is with the Departamento de Sistemas Telemáticos y Computación, University Rey Juan Carlos, 28933 Móstole, Spain.

Digital Object Identifier 10.1109/TCSII.2008.921426

II. SYSTEM DESCRIPTION

The chaos-coded modulator accepts as input an identically and independently distributed (*i.i.d.*) bit sequence $b_n \in \{0, 1\}$, and produces a chaos-coded sequence, based on switched chaotic maps driven by small perturbations [1], [2], following:

$$\begin{aligned} z_n &= f(z_{n-1}, b_n) + b_n \cdot 2^{-Q} \\ x_n &= g(z_n) = 2z_n - 1 \end{aligned} \quad (1)$$

where $f(\cdot, 0) = f_0(\cdot)$ and $f(\cdot, 1) = f_1(\cdot)$ are chaotic maps that leave the interval $[0, 1]$ invariant. They are piecewise-linear maps with slope ± 2 . The natural number Q controls the amplitude of the small perturbation term, so that it manifests itself after $Q - 1$ iterations. It has been shown that this kind of encoder leaves a set $S_Q = \{i \cdot 2^{-Q} | i = 0, \dots, 2^Q - 1\}$ of 2^Q points invariant [1], so that, when taking as initial condition a point from S_Q (e.g., $z_0 = 0$), z_n will lie in S_Q . In this way, we have a quantized chaotic sequence x_n over 2^Q values.

We consider the following pairs of maps $f_0(\cdot)$ and $f_1(\cdot)$.

1) Bernoulli shift map (BSM)

$$f_0(z) = f_1(z) = 2z \bmod 1. \quad (2)$$

2) Tent map (TM)

$$f_0(z) = f_1(z) = \begin{cases} 2z, & 0 \leq z < \frac{1}{2} \\ 2 - 2z, & \frac{1}{2} \leq z \leq 1. \end{cases} \quad (3)$$

3) The BSM and its shifted version (multi-BSM, mBSM)

$$f_0(z) = 2z \bmod 1 \quad (4)$$

$$f_1(z) = \begin{cases} 2z + \frac{1}{2}, & 0 \leq z < \frac{1}{4} \\ 2z - \frac{1}{2}, & \frac{1}{4} \leq z < \frac{3}{4} \\ 2z - \frac{3}{2}, & \frac{3}{4} \leq z \leq 1. \end{cases} \quad (5)$$

4) The TM and its shifted version (multi-TM, mTM)

$$f_0(z) = \begin{cases} 2z, & 0 \leq z < \frac{1}{2} \\ 2 - 2z, & \frac{1}{2} \leq z \leq 1 \end{cases} \quad (6)$$

$$f_1(z) = \begin{cases} 2z + \frac{1}{2}, & 0 \leq z < \frac{1}{4} \\ 2z - \frac{1}{2}, & \frac{1}{4} \leq z < \frac{3}{4} \\ \frac{3}{2} - 2z, & \frac{1}{2} \leq z < \frac{3}{4} \\ \frac{5}{2} - 2z, & \frac{3}{4} \leq z \leq 1. \end{cases} \quad (7)$$

In Fig. 1, we have depicted them. These CCM systems, when restricted to S_Q , allow an equivalent representation in terms of a *trellis encoder*, where the transitions are driven by the input bit b_n . Therefore, such CCM systems are closely related to TCM

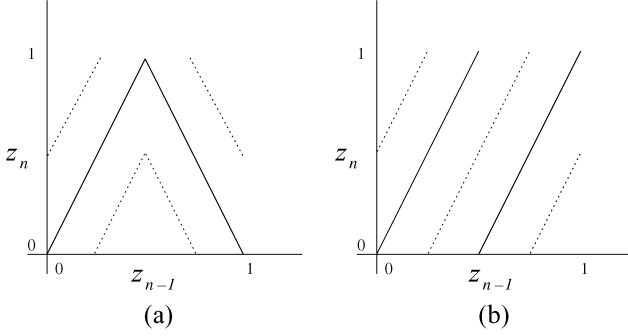


Fig. 1. Maps for the CCM encoders. Continuous line: $f_0(\cdot)$. Dotted line: $f_1(\cdot)$. (a) mTM (continuous line: TM). (b) mBSM (continuous line: BSM).

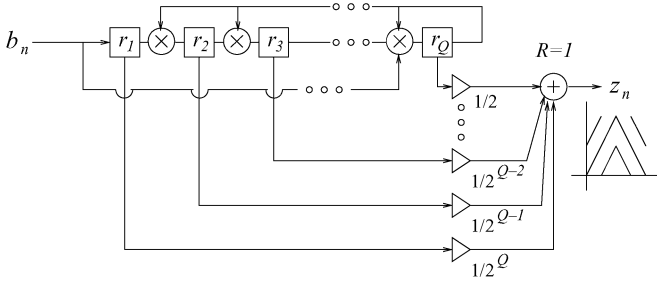


Fig. 2. Finite-state encoding structure for the mTM CCM.

systems with rate $R = 1$ bit/symbol[1]. In Fig. 2, we can see the equivalent trellis encoder for the mTM CCM.

The channel is affected by fast flat fading [6]. It is described by an uncorrelated sequence of amplitudes a_n which follow a Rician probability density function (pdf) given by

$$p(a_n) = 2a_n(1+K)e^{-a_n^2(1+K)-K} I_0\left(2a_n\sqrt{K(K+1)}\right)$$

where $I_0(\cdot)$ is the zeroth-order modified Bessel function of the first kind, K is the ratio of specular to diffuse energy [6], and $a_n \geq 0$. $K = 0$ corresponds to the Rayleigh case, and $K \rightarrow \infty$, to no fading. The mean and variance are given by

$$\eta_a = \frac{1}{2} \sqrt{\frac{\pi}{1+K}} e^{-\frac{K}{2}} \left[(1+K)I_0\left(\frac{K}{2}\right) + KI_1\left(\frac{K}{2}\right) \right]$$

$$\sigma_a^2 = 1 - \eta_a^2$$

where $I_1(\cdot)$ is the first-order modified Bessel function of the first kind. $E[a_n^2] = 1$, so that the signal to noise ratio is not affected. The channel is further described by AWGN, which adds *i.i.d.* Gaussian samples n_n with mean 0 and power σ^2 .

Due to the trellis coded properties of the signal, the receiver can be designed by using *maximum likelihood* (ML) or *maximum a posteriori* (MAP) sequence decoding algorithms. In this case, we have used a known MAP soft-input soft-output (SISO) decoder adapted to the decoding of this kind of chaotic sequences in the AWGN channel [7]. We do not review the details of this SISO module here. We point out instead the needed arrangements for the flat fading channel. The SISO decoder takes as input a block of M received samples

$$r_n = y_n + n_n = a_n x_n + n_n, \quad n = 1, \dots, M. \quad (8)$$

To process them, the channel metrics have to be adapted to the two possible situations respecting the knowledge of the channel state at the decoder. In the best situation, the sequence of fading

amplitudes $\mathbf{a} = (a_1, \dots, a_M)$ is known due to the presence of a channel-estimation method [channel-state information (CSI) case]. In this situation, the SISO decoding algorithm uses the metric $(r_n - a_n x_n)^2$ [6]. In the other case, the receiver has only information, if any, about some parameters of the channel, such as the mean η_a (case without CSI). Now the metric for the SISO decoding algorithm is taken as $(r_n - \eta_a x_n)^2$ [8].

III. PERFORMANCE ANALYSIS

There will be an error event when having sent the sequence \mathbf{x} , the decoder chooses $\mathbf{x}' \neq \mathbf{x}$, both sequences starting in the same state and merging again in (possibly) other state after L steps.¹ Assuming ML decoding² and using the mentioned channel metrics, this is equivalent to

$$\sum_{n=m}^{L+m-1} (r_n - a_n x'_n)^2 < \sum_{n=m}^{L+m-1} (r_n - a_n x_n)^2 \quad (9)$$

for the perfect CSI case, and

$$\sum_{n=m}^{L+m-1} (r_n - \eta_a x'_n)^2 < \sum_{n=m}^{L+m-1} (r_n - \eta_a x_n)^2 \quad (10)$$

without CSI [6]. After some algebra, we get the inequalities

$$\sum_{n=m}^{L+m-1} a_n^2 (x_n - x'_n)^2 = A$$

$$\leq 2 \sum_{n=m}^{L+m-1} n_n a_n (x_n - x'_n) \quad \text{with CSI} \quad (11)$$

$$\sum_{n=m}^{L+m-1} \left[(a_n x_n - \eta_a x_n)^2 - (a_n x'_n - \eta_a x'_n)^2 \right] = B$$

$$\leq 2\eta_a \sum_{n=m}^{L+m-1} n_n (x_n - x'_n) \quad \text{without CSI} \quad (12)$$

where A and B are random variables (RVs) whose meaning will be clear in the sequel. The right-hand side members of (11) and (12) are Gaussian RVs because they are weighted sums of independent Gaussian RVs. x_n, x'_n, a_n , and η_a are assumed to be known in this step, since we are calculating the conditioned pairwise-error probability (PEP). Therefore, the PEPs conditioned to the fading amplitudes are [6]

$$P_e^{\text{w/CSI}}(\mathbf{x} \rightarrow \mathbf{x}' | \mathbf{x}, \mathbf{a}) = \frac{1}{2} \operatorname{erfc} \left(\sqrt{\frac{1}{4P} \frac{E_b}{N_0} A} \right)$$

$$\leq \frac{1}{2} \exp \left(-\frac{1}{4P} \frac{E_b}{N_0} A \right) \quad (13)$$

$$P_e^{\text{w/oCSI}}(\mathbf{x} \rightarrow \mathbf{x}' | \mathbf{x}, \mathbf{a}) = \frac{1}{2} \operatorname{erfc} \left(\sqrt{\frac{1}{4P} \frac{E_b}{N_0} \frac{B}{\eta_a d_E}} \right)$$

$$\leq \frac{1}{2} \exp \left(-\frac{1}{4P} \frac{E_b}{N_0} \frac{B^2}{\eta_a^2 d_E^2} \right) \quad (14)$$

¹Note that the error events cannot be simply calculated by supposing having sent the all zero codeword, since these systems are nonlinear. We are also assuming implicitly that $L \ll M$.

²Since the *a priori* probabilities of b_n are the same, MAP decoding is equivalent to ML decoding.

where $d_E^2 = \sum_{n=m}^{L+m-1} (x_n - x'_n)^2$ is the squared Euclidean distance between \mathbf{x} and \mathbf{x}' , $P = 1/3$ is the power of the chaos modulated signal,³ and $E_b/N_0 = 2P/\sigma^2$ is the signal to noise ratio in terms of the ratio of bit energy to noise power-spectral density. We have also made use of $\text{erfc}(x) \leq \exp(-x^2)$ [9].

Taking into account the fact that A is a sum of noncentral χ^2 RVs with known statistics, and B , for $L \geq 5$, a Gaussian RV by virtue of the Central Limit Theorem [9], the unconditioned PEPs can be upper bounded by

$$\begin{aligned} P_e^{\text{wCSI}}(\mathbf{x} \rightarrow \mathbf{x}'|\mathbf{x}) &= E_{\mathbf{a}} [P_e^{\text{wCSI}}(\mathbf{x} \rightarrow \mathbf{x}'|\mathbf{x}, \mathbf{a})] \\ &\leq \frac{1}{2} \prod_{n=m}^{L+m-1} \frac{1+K}{1+K + \frac{1}{4P} \frac{E_b}{N_0} (x_n - x'_n)^2} \\ &\quad \times \exp\left(-\frac{K \frac{1}{4P} \frac{E_b}{N_0} (x_n - x'_n)^2}{1+K + \frac{1}{4P} \frac{E_b}{N_0} (x_n - x'_n)^2}\right) \end{aligned} \quad (15)$$

$$\begin{aligned} P_e^{\text{w/oCSI}}(\mathbf{x} \rightarrow \mathbf{x}'|\mathbf{x}) &= E_{\mathbf{a}} [P_e^{\text{w/oCSI}}(\mathbf{x} \rightarrow \mathbf{x}'|\mathbf{x}, \mathbf{a})] \\ &\leq \frac{1}{2} \frac{1}{\sqrt{1 + \frac{2}{P} \frac{E_b}{N_0} \sigma_a^2 \frac{\theta(\mathbf{x}, \mathbf{x}')}{d_E^2}}} \\ &\quad \times \exp\left(-\frac{\frac{1}{4P} \frac{E_b}{N_0} \eta_a^2 d_E^2}{1 + \frac{2}{P} \frac{E_b}{N_0} \sigma_a^2 \frac{\theta(\mathbf{x}, \mathbf{x}')}{d_E^2}}\right). \end{aligned} \quad (16)$$

There, we have defined

$$\theta(\mathbf{x}, \mathbf{x}') = \sum_{n=m}^{L+m-1} x_n^2 (x_n - x'_n)^2 \leq \sum_{n=m}^{L+m-1} (x_n - x'_n)^2 = d_E^2.$$

Note that (16) tends to 0 when $E_b/N_0 \rightarrow \infty$, but the simulations will show an error floor. This can be accounted for seeing that the right-hand side member of (12) is only affected by noise for fixed \mathbf{x} and \mathbf{x}' . This term becomes negligible when the noise power is much lower than the signal power,⁴ so that the error event will only depend on a_n , following:

$$2 \sum_{n=m}^{L+m-1} a_n \eta_a x_n (x_n - x'_n) \leq \eta_a^2 \sum_{n=m}^{L+m-1} (x_n^2 - x'_n{}^2). \quad (17)$$

Using the fact that the left-hand side member of (17) is again a Gaussian RV for $L \geq 5$, we arrive at

$$P_{\text{error}}^{\text{w/oCSI}}(\mathbf{x} \rightarrow \mathbf{x}'|\mathbf{x}) \rightarrow \frac{1}{2} \text{erfc}\left(\frac{\eta_a d_E^2}{2\sigma_a \sqrt{2\theta(\mathbf{x}, \mathbf{x}')}}\right). \quad (18)$$

A. BEP With CSI

To give a bound for the bit-error probability (BEP), we have to analyze the most probable pairwise-error events and the related binary error events. In (15) we see that the most probable pairwise-error events when $E_b/N_0 \rightarrow \infty$ will be those with

minimum $(x_n - x'_n)^2$, $n = m, \dots, L+m-1$. These error events will be the ones leading to minimum d_E^2 for the kind of CCMS seen here.⁵ In the case of BSM,⁶ such binary error events have length $L = Q+1$ and are of the type $b_m, b_{m+1}, \dots, b_{m+Q}$ vs $b_m^*, b_{m+1}^*, \dots, b_{m+Q}^*$, with $b_m \neq b_m^*$. Thus, the associated binary error event is $\mathbf{e} = \mathbf{b} \otimes \mathbf{b}' = (1, (Q-1 \text{ 0's}), 0)$, and has Hamming weight $w(\mathbf{e}) = 1$. It leads to $(x_n - x'_n)^2 = (1/4)^{m+Q-n}$, $n = m, \dots, m+Q-1$ [1], with independence of previous values of b_n and x_n , so that

$$P_b^{\text{wCSI}} \approx \beta_{\min} \frac{1}{2} \prod_{i=0}^{Q-1} \frac{1+K}{1+K + \frac{1}{4P} \frac{E_b}{N_0} \frac{1}{4^i}} \cdot \exp\left(-\frac{K \frac{1}{4P} \frac{E_b}{N_0} \frac{1}{4^i}}{1+K + \frac{1}{4P} \frac{E_b}{N_0} \frac{1}{4^i}}\right) \quad (19)$$

where $\beta_{\min} = 1$ is the bit enumerator of these error events.

In the rest of CCMS seen (mBSM, TM, mTM), since they not comply with the uniform error event property [6], the error events associated with minimum d_E^2 lead to different values for $(x_n - x'_n)^2$ depending on the exact values of x_n and x'_n . The mBSM CCM has the same kind of binary input errors events leading to minimum d_E^2 as the BSM CCM (i.e., $L = Q+1$ and $w(\mathbf{e}) = 1$), while for the TM and the mTM CCM we have the input binary error events with $L = Q+1$, $w(\mathbf{e}) = Q$ and $\mathbf{e} = (1, (Q-1 \text{ 1's}), 0)$. To calculate the bound, it is enough to consider the 2^Q equiprobable possible values for x_m , and the 2^L equiprobable possible values for b_m, \dots, b_{m+L-1} , because the rest of values of x_n and x'_n are determined by them and by the binary error event \mathbf{e} associated to each CCM.

Now, taking into account that there will be 2^{Q+L} equiprobable sequences $(x_n - x'_n)^2$, $n = m, \dots, m+L-1$, related to such error event, the average bound for $E_b/N_0 \rightarrow \infty$ is

$$P_b^{\text{wCSI}} \approx \frac{\beta_{\min}}{2^{Q+L}} \sum_{\mathbf{x}, \mathbf{x}'} P_e^{\text{wCSI}}(\mathbf{x} \rightarrow \mathbf{x}'|\mathbf{x}) \quad (20)$$

where the summation is taken over such 2^{Q+L} different sequences $\mathbf{x} = (x_m, \dots, x_{m+L-1})$, $\mathbf{x}' = (x'_m, \dots, x'_{m+L-1})$, $P_e^{\text{wCSI}}(\mathbf{x} \rightarrow \mathbf{x}'|\mathbf{x})$ is as seen in (15) and β_{\min} is 1 for the mBSM CCM, and Q for the TM and mTM CCMS. Note that, due to the structure of (15), one could think of managing the final error rate by increasing Q and thus the loop length L . Nevertheless, as seen in the case of the BSM [bound (19)], the terms $(x_n - x'_n)^2$ decrease with increasing powers of $1/4$, so that there exists a tradeoff and the result is almost insensitive to Q . This happens also with the rest of CCMS proposed here, since, due to the ± 2 map slope, $(x_n - x'_n)^2$ will also decrease with increasing powers of $1/4$ [1].

B. BEP Without CSI

The analysis is more involved without CSI, since, as seen in (16) and (18), the PEP depends on the exact values of x_n through $\theta(\mathbf{x}, \mathbf{x}')$. Nevertheless, the bound can still be calculated with the error events associated with the minimum of d_E^2 , since $\theta(\mathbf{x}, \mathbf{x}') \leq d_E^2$. We have again 2^Q equiprobable possible values for x_m , and 2^L possible input sequences b_m, \dots, b_{m+L-1} . Each

³All these CCMS generate uniformly distributed chaotic samples within $[-1, 1]$. $P = 1/3$ for $Q \rightarrow \infty$, but, if $Q \geq 4$, the difference is negligible.

⁴Specially when K is small and the dispersion of the values a_n is high.

⁵Such error events correspond to the ones with minimum loop length L .

⁶For BSM, $d_{E_{\min}}^2 = 4/3$ if $Q \rightarrow \infty$. It is a good approximation if $Q \geq 4$.

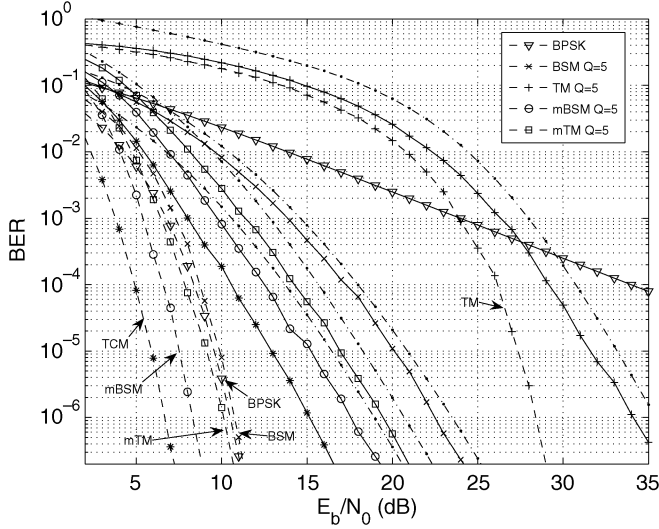


Fig. 3. Results in Rayleigh fading with CSI (continuous lines), for BSM, TM, mBSM, and mTM CCMs with $Q = 5$, and for TCM (*). '∇': BPSK bounds. Marked with arrows: results in AWGN. Dash-dotted line at the right of each CCM curve is the corresponding bound.

of these sequences is equiprobable, so that, in the midrange E_b/N_0 region where (16) is valid, the average BEP associated with such error events will be

$$P_b^{w/oCSI} \approx \frac{\beta_{\min}}{2Q+L} \frac{1}{2} \sum_{\mathbf{x}, \mathbf{x}'} \frac{1}{\sqrt{1 + \frac{2}{P} \frac{E_b}{N_0} \sigma_a^2 \frac{\theta(\mathbf{x}, \mathbf{x}')}{d_E^2}}} \cdot \exp \left(- \frac{\frac{1}{4P} \frac{E_b}{N_0} \eta_a d_E^2}{1 + \frac{2}{P} \frac{E_b}{N_0} \sigma_a^2 \frac{\theta(\mathbf{x}, \mathbf{x}')}{d_E^2}} \right) \quad (21)$$

where \mathbf{x} , \mathbf{x}' and β_{\min} are as in the CSI case. When $E_b/N_0 \rightarrow \infty$ and we are in the error floor region, we get

$$P_{b_{\text{floor}}}^{w/oCSI} \approx \frac{\beta_{\min}}{2Q+L} \frac{1}{2} \sum_{\mathbf{x}, \mathbf{x}'} \operatorname{erfc} \left(\frac{\eta_a d_E^2}{2\sigma_a \sqrt{2\theta(\mathbf{x}, \mathbf{x}')}} \right). \quad (22)$$

IV. SIMULATION RESULTS AND DISCUSSION

In Figs. 3 and 4, we can see the simulation results and bounds for fading with CSI. For comparison, we have depicted the bounds for binary phase-shift keying (BPSK) [6], and simulation results for a conventional $R = 1$ bit/symbol TCM scheme consisting on a constraint length $\nu = 5$ encoder with polynomials 06 and 23 and quadrature phase-shift keying (QPSK) modulation [10]. It is a rotationally invariant system suitable for fading channels. All simulations have been run with a block length of $M = 10^5$ symbols.

Though the CCMs seen, excepting the TM CCM, exhibit performances close to BPSK in AWGN, in presence of fading their coded nature leads to much lower losses. This means that they can keep the good properties of coded modulations in fading [6]. Note that the TM case is the worst in BER, but it also has the lowest losses in Rayleigh fading with CSI. In Fig. 4, we verify how the Rician channel tends to the AWGN one when $K \rightarrow \infty$, and that there is a steady coding gain with respect to uncoded

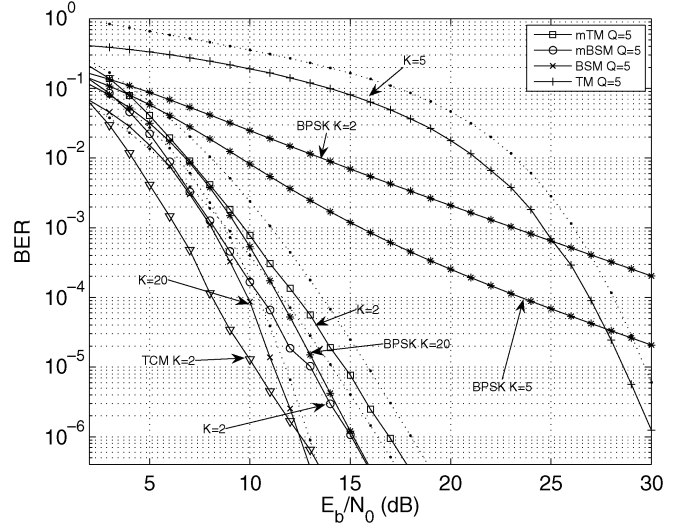


Fig. 4. Results in Rician fading with CSI (continuous lines), for BSM, TM, mBSM, and mTM CCMs with $Q = 5$. '*': BPSK bounds. '∇': TCM results with $K = 2$. Dotted lines at the right of each CCM curve are the bounds.

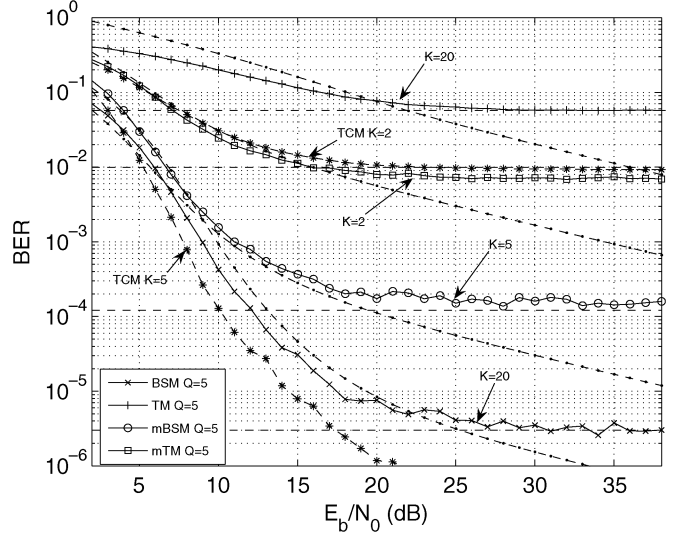


Fig. 5. Results in Rician fading without CSI, for BSM, TM, mBSM, and mTM CCMs with $Q = 5$. Dashed horizontal line close to each CCM curve: error floor bound. Dash-dotted line: bound of (21). '*': results for TCM.

BPSK. Moreover, the bounds shown in Figs. 3 and 4 are good enough to give reason of the BER for high E_b/N_0 . Note that the best CCMs shown, mBSM and mTM, exhibit losses in the fading channel with respect to the AWGN channel that are comparable to the losses of the conventional TCM system: for $K = 0$, the losses for a BER of 10^{-5} lie always around 7 dB, and for $K = 2$, around 4.5 dB.

In Fig. 5, we plot the results without CSI. Note the presence of an error floor whose value diminishes when $K \rightarrow \infty$. For K high enough to have a distinct waterfall region, the bound of (21) shows to be accurate enough, while the bound of (22) gives a very tight approximation to the error floor. Note that the TCM and the mTM systems have the same performance for $K = 2$, while, for $K = 5$, the TCM clearly outperforms all the CCMs. This points towards a potential advantage of the CCMs with respect to conventional TCM when there is no CSI and the channel tends to a Rayleigh one.

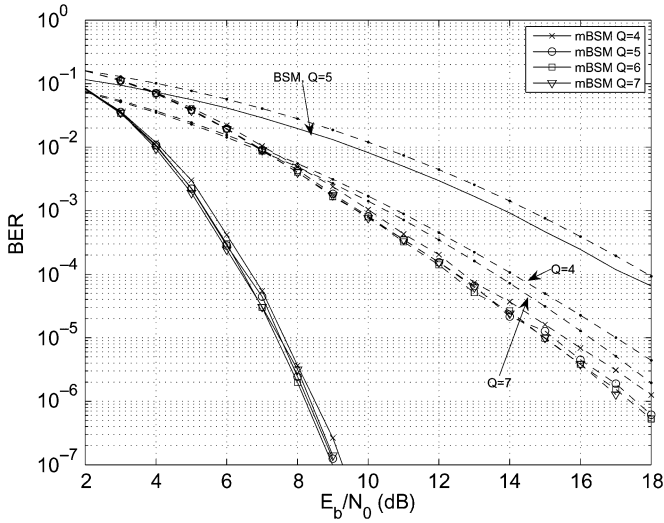


Fig. 6. Results in AWGN (continuous lines) and Rayleigh fading with CSI (dashed lines), for mBSM with different Q . Dash-dotted lines over the mBSM results are bounds for $Q = 4$ and $Q = 7$. Upper continuous line: BSM results for $K = 0$ with $Q = 5$. Upper dash-dotted line: BSM bound with $Q = 100$.

It is known that, in fading channels with CSI, TCMs should be designed with the largest minimum error loop length L , and with the highest product distance $(\prod_{n=m}^{m+L-1} (x_n - x'_n)^2)$ [6]. In the case without CSI, the behavior of TCM is dominated by the minimum Euclidean distance [6]. This is a difference with respect to our kind of CCM. As pointed out by the bounds, the loop length L can be virtually made as high as desired just by increasing Q , while the product distance tends to 0. The Euclidean distance remains bounded with $L \rightarrow \infty$ [1], and thus $\theta(\mathbf{x}, \mathbf{x}')$. Due to all this, we can foresee that these CCMs will be relatively insensitive to Q . In Fig. 6, we have plotted several curves with different Q . The results and the bounds for the mBSM CCM, both in the AWGN channel and in the Rayleigh fading channel with CSI, show that the effect of Q is small, provided that $Q \geq 5$. The results for the BSM CCM with $Q = 5$ in the Rayleigh channel with CSI, when compared with the bound depicted for the same case with $Q = 100$ [using (19)], stress this relative insensitivity.⁷ Though not shown, this property holds without CSI. Thus, in practice Q can be kept low (the decoder works over 2^Q states), while preserving the properties of the $Q \rightarrow \infty$ case.⁸

Taking all this into account, we can say that the behavior of these kind of chaos-based systems does not rely on conventional parameters, like loop length, product distance or Euclidean distance. They rely instead on the complex structure introduced in the spectrum of symbolic distances $(x_n - x'_n)^2$ and $x_n^2(x_n - x'_n)^2$ for the class of most probable error events, and this depends on the structure of the chaotic maps involved. Moreover, we have seen that the BSM offers regularity but it is not useful, while the TM is a pathological system [1], but we have verified that, introducing them in a switched map scheme, we can get gains in AWGN and fading. We have thus achieved

⁷This bound is feasible thanks to the quasi-linear structure of BSM.
⁸Note that $Q = 5$ is the lowest value for the bounds to be useful, since $L = Q + 1 > 5$ was assumed in the calculations.

a positive modification in the spectrum of said symbolic distances. This is equivalent to focusing on multiplicities of error events rather than just on distances, and this is precisely the philosophy of successful turbocodes [8].

V. CONCLUSION

We have developed here some bounds for a kind of CCMS based on switched chaotic maps driven by small perturbations, and we have shown that these bounds, when considering a limited number of error events, can be useful to estimate the final performance of the system. We have also shown that, in case of perfect CSI, these CCMS can offer in general a steady coding gain with respect to uncoded BPSK, even when in the AWGN channel could be the opposite, while exhibiting a degradation not worse than with conventional TCM systems. When no CSI is available, we have verified the appearance of an error floor and a much poorer behavior, so that in this case these modulations require diversity strategies to be of potential use. Nevertheless, CCM systems have shown a relative advantage with respect to conventional TCM in the quasi-Rayleigh channel without CSI. One of the main advantages of the chaos based signals used, together with the fact that the encoder allows a very simple implementation, is that they offer the same performance with independence of the quantization level, provided that it is higher than a minimum, but that can be kept low enough to make MAP or ML sequence decoding feasible. In this way, the bounds can be managed statistically with the $Q \rightarrow \infty$ case, and made useful in design and evaluation tasks. It has been shown that chaos-based techniques can be most useful in environments where the statistical properties of the signals are the dominant factor [5], and this allows us to foresee the possibility to build good performing CCM systems in the fading channel with the help of the principles and tools shown.

REFERENCES

- [1] S. Kozić, T. Schimming, and M. Hasler, "Controlled one- and multidimensional modulations using chaotic maps," *IEEE Trans. Circuits Syst. I, Reg. Papers*, vol. 53, no. 9, pp. 2048–2059, Sep. 2006.
- [2] F. J. Escribano, L. López, and M. A. F. Sanjuán, "Parallel concatenated chaos-coded modulations," in *Proc. Int. Conf. Software, Telecomm. Comput. Netw.*, Split-Dubrovnik, Croatia, Sep. 2007.
- [3] W. M. Tam, F. C. M. Lau, and C. K. Tse, *Digital Communications With Chaos*. Oxford, U.K.: Elsevier, 2007.
- [4] Y. Xia, C. K. Tse, and F. C. M. Lau, "Performance of differential chaos-shift-keying digital communication systems over a multipath fading channel with delay spread," *IEEE Trans. Circuits Syst. II, Exp. Briefs*, vol. 51, no. 12, pp. 680–684, Dec. 2004.
- [5] G. Mazzini, R. Rovatti, and G. Setti, "Chaos-based asynchronous DS-CDMA systems and enhanced rake receivers: Measuring the improvements," *IEEE Trans. Circuits Syst. I, Fundam. Theory Appl.*, vol. 48, no. 12, pp. 1445–1453, Dec. 2001.
- [6] M. K. Simon and M.-S. Alouini, *Digital Communications over Fading Channels*. Hoboken, NJ: Wiley, 2005.
- [7] F. J. Escribano, L. López, and M. A. F. Sanjuán, "Iteratively decoding chaos encoded binary signals," in *Proc. Int. Symp. Signal Processing Appl.*, Sydney, Australia, Aug. 2005, vol. 1, pp. 275–278.
- [8] E. K. Hall and S. G. Wilson, "Design and analysis of turbo codes on Rayleigh fading channels," *IEEE J. Sel. Areas Commun.*, vol. 16, no. 2, pp. 160–174, Feb. 1998.
- [9] A. Papoulis and S. U. Pillai, *Probability, Random Variables and Stochastic Processes*. Boston, MA: McGraw-Hill, Inc., 2002.
- [10] S. Lin and D. J. Costello, Jr, *Error Control Coding*. Upper Saddle River, NJ: Prentice-Hall, 2004.